High-Performance Metal Organic Cluster Resists for High-NA Extreme Ultraviolet Lithography

Manvendra Chauhan[1], Neha[1], Kumar Palit,[1] Ranbir Singh[2], Abhimanew Dhir[3], Robin Khosla[1], Bhaskar Mondal[3], Satinder K. Sharma*[1]
&
Ralph Dammel[4], Ravi Kanjolia[4]

1 School of Computing & Electrical Engineering (SCEE), 2 School of Mechanical and Materials Engineering (SMME), 3 School of Chemical Sciences (SCS), Indian Institute of Technology (IIT), Mandi, MANDI-175075, (Himachal Pradesh), India &
4 EMD Electronics, 70 Meister Ave, Somerville, NJ 08876

Presenting Author E-mail: ***ralph.dammel@merckgroup.com****;satinder@iitmandi.ac.in*

Abstract

High-NA EUV lithography stands at the forefront of enabling single-digit technology nodes in high-volume chip manufacturing (HVCM), representing a transformative leap in the semiconductor industry. To harness this, it is essential to develop unique nano metal-organic clusters (nMOCs) resists that can effectively address the challenges of high resolution, sensitivity, roughness, stochastic effects, and trade-offs. nMOCs can remarkably pattern high-resolution features below 15 nm with low line-edge roughness (LER) and exceptional EUV sensitivity ($\lambda \sim$ 13.5 nm), ascribed to innovative integration of metal cores and ligands, which enhances performance. On the other hand, elevated sensitivity can compromise resolution due to excessive energy absorption, resulting in HR pattern blurring and proximity effects, over-exposing unintended resist areas. This study seeks to pioneer the development of cutting-edge Indium (In) based nMOCs resists pre-screened through electron beam lithography (EBL) & helium ion beam lithography (HIBL) and prelude for EUVL. The key to overcoming these challenges lies in the strategic design of ligands for QSAR characteristics and absorptivity. Focusing, these efforts can drive significant advancements in lithography technology, ensuring the future of high-performance chip manufacturing.

Keywords: High-resolution patterning, high-NA EUV, lithography.

1. INTRODUCTION

As semiconductor technology progresses toward sub-10 nm device architectures, high-numerical aperture (high-NA) extreme ultraviolet lithography (EUVL) has become a key enabler for fabricating next-generation features at this scale. The demand for high-NA EUVL emerged due to the limitations of conventional photolithography, which struggles to achieve the critical dimension (CD) scaling necessary for advanced logic and memory applications. High-NA EUVL enables superior resolution by minimizing the diffraction-limited feature sizes. However, realizing this technology involves formidable challenges, particularly in developing EUV-compatible resists that can deliver the required sensitivity, resolution, and low line-edge roughness (LER)[1].

A major challenge in EUV resist development lies in balancing sensitivity and resolution while mitigating LER and line-width roughness (LWR). Commercially available chemically amplified resists (CARs), primarily based on organic polymeric formulations, often suffer from inadequate EUV photon absorption, leading to stochastic effects and patterning defects at sub-10 nm dimensions. Moreover, CARs exhibit poor etch resistance, limiting their integration into advanced EUV lithographic processes[2]. This situation has driven significant research into alternative high-absorption resist platforms, particularly focusing on inorganic and hybrid organic-inorganic resists, with metal-organic clusters (MOCs) emerging as a promising category[3–6].

Recent studies have explored MOC-based EUV resists, revealing enhanced performance in high-resolution nanopatterning due to their high etch resistance, improved EUV absorption, and superior mechanical stability. Indium-based metal-organic cluster (MOC) resists, particularly In-MAA resist, have shown promising lithographic performance under high-NA EUV exposure, exhibiting ultra-sensitivity towards EUV photons, improved resolution and lower LER compared to traditional

Advances in Patterning Materials and Processes XLII, edited by Ryan Callahan, Anuja De Silva, Proc. of SPIE Vol. 13428, 1342809 · © 2025 SPIE
0277-786X · doi: 10.1117/12.3052190

polymer-based CARs and inorganic resists[6]. Among MOC-based resists, indium-based clusters have gained significant attention due to their high EUV absorption cross-section[7], excellent stability, and tunable ligand chemistry. The choice of organic ligand in MOCs plays a critical role in determining solubility, pattern contrast, and etch resistance. m-Toluic acid (mTA), with its aromatic structure and carboxylate functionality, offers a potentially robust ligand for indium-based MOCs, promoting enhanced resist solubility, strong metal-ligand binding, and improved pattern fidelity. Additionally, the methyl substitution in mTA can provide tailored resist dissolution kinetics, optimizing contrast and sensitivity during EUV and e-beam lithographic processing[5].

In this study, we designed and synthesized a new class of indium-based metal-organic cluster (In-mTA MOC) resists, incorporating 2-iodopropane as an additive to enhance lithographic performance. These formulations were developed to achieve higher sensitivity, improved resolution, and optimized pattern development, making them suitable for high-resolution electron beam lithography (EBL) and helium ion beam lithography (HIBL), which serve as prototyping techniques for extreme ultraviolet lithography (EUVL). A systematic evaluation of their lithographic characteristics was conducted, including contrast curve analysis, line-edge roughness (LER) measurements, and sub-15 nm patterning capabilities under both EBL and HIBL exposures. Additionally, the role of 2-iodopropane in improving resist solubility and sensitivity was investigated, demonstrating its effectiveness in enhancing contrast and resolution for advanced nanolithographic applications.

2. EXPERIMENTAL SECTION

Materials: Indium (III) acetate, m-Toluic acid, triethylamine, acetylacetone, and 2-iodopropane were procured from Sigma-Aldrich. Ethyl acetate and 1-propanol were obtained from S D Fine Chemicals (SDFCL), while ethyl lactate was sourced from TCI Chemicals.

2.1 Synthesis of metal organic cluster (MOC) resist

The In-MOC resist materials were synthesized via a sol-gel process, ensuring controlled reaction conditions for optimal complex formation. In the first step, Indium (III) acetate was dissolved in ethyl acetate, producing a uniform and homogeneous precursor solution (Solution A). Concurrently, mTA, trimethylamine, and ethyl acetate were combined to create Solution B, facilitating ligand-metal interaction. To promote a well-defined cluster formation, Solution B was gradually introduced dropwise into Solution A at 70°C, while continuously stirring the mixture to maintain homogeneity and reaction efficiency. The reaction was allowed to proceed for 12 hours at 70°C, ensuring the complete formation of the indium-ligand coordination complex. After synthesis, the resulting material underwent a series of ethanol washes to remove any unreacted precursors and byproducts. The purified product was then subjected to thermal drying in an oven at 50°C for 4 hours to eliminate residual solvents. The final resist obtained in a gel form was carefully stored in a vacuum desiccator to preserve its stability and prevent moisture-induced degradation, ensuring its suitability for further lithographic applications.

2.2 Resist formulation and thin film preparation

A 2.5 wt.% solution of the synthesized In-mTA resist was prepared by dissolving it in ethyl lactate using a vortex mixer to ensure uniform dispersion. To introduce iodine doping, 2-iodopropane was selected as the iodine source and incorporated into the resist formulations at two distinct concentrations: 2 v/v% and 4 v/v%. The resist formulation without iodine doping was designated as R1, while the formulations containing 2 v/v% and 4 v/v% 2-iodopropane were referred to as R2 and R3, respectively.

For thin-film deposition, each resist solution was spin-coated at 3000 rpm for 45 seconds onto an RCA-cleaned silicon wafer, forming a uniform resist layer. The coated films were then subjected to a prebake at 90°C for 60 seconds removing residual solvents and th film thickness was measures as ~ 28 nm. The post-exposure bake (PEB) temperature was also maintained at 90°C for 60 seconds, ensuring proper resist crosslinking and development compatibility.

2.3 Electron beam lithography (EBL): Conducted using the e-Line PLUS system (Raith GmbH, Dortmund, Germany), where a high-precision 18 keV electron beam was employed to expose a ~28 nm-thick resist layer. The process was carried out at a beam current of approximately 17.4 pA, utilizing a 10 µm aperture, with a controlled range of electron doses to achieve optimal patterning conditions.

2.4 Helium ion Beam Lithography (He^+BL): Carried out using the Zeiss ORION NanoFab system, where a 30 keV He^+ ion beam was directed onto a ~28 nm-thick resist layer at a beam current of approximately 0.25 pA, utilizing a 20 µm numerical aperture for precise patterning.

Following exposure to both He^+ beam and electron beam, the negative tone patterns were developed in a 1-propanol and acetylacetone mixture, with the exposed thin films being immersed for 30 seconds, followed by a 10-second rinse in isopropanol (IPA) to ensure proper pattern development.

2.5 Characterization

To analyze the resist nano-patterning, Field Emission Scanning Electron Microscopy (FESEM, Zeiss Gemini SEM 500, Germany) was utilized, enabling high-resolution imaging to assess the pattern feature width and uniformity. The identification of surface functional groups was conducted through Fourier Transform Infrared Spectroscopy (FTIR) using a Cary 600 Series spectrometer, which provided insights into the chemical bonding and molecular interactions within the resist formulation. The film thickness of the deposited resist layers was measured with an Atomic Force Microscope (AFM, Bruker Icon), ensuring precise evaluation of uniformity and consistency across the coated substrate. Additionally, line-edge roughness (LER) and line-width roughness (LWR) of the exposed line patterns were systematically quantified using SuMMIT® metrology software, a widely recognized industry standard for evaluating pattern fidelity and nanoscale roughness in lithographic processes.

3. RESULTS AND DISCUSSION

The lithographic performance of the pristine In-mTA MOC resist formulations, along with those incorporating 2 v/v% and 4 v/v% 2-iodopropane, was evaluated using EBL and HIBL as a preliminary assessment for EUV lithography.

3.1 High-resolution pattern analysis for In-mTA MOC resists

To achieve well-resolved sub-15 nm patterning, freshly prepared In-mTA MOC resists (R1, R2, and R3), spin-coated to a thickness of approximately 28 nm, were initially exposed to electron beam lithography (EBL) across a broad range of exposure doses. Following e-beam exposure, the resist samples underwent pattern development in a solution of 1-propanol and acetylacetone. The resulting line-pattern features and development quality were subsequently analyzed using FESEM.

3.1.1 Lithographic Performance of R1 Resist (Pristine In-mTA MOC)

After the EBL patterning, the R1 resist demonstrated potential for sub-15 nm line patterning at the e-beam exposure dose of ~ 1012 µC/cm^2. However, for sub-20 nm half-pitch (HP) line-patterns, resist residue and pattern bridging were observed, indicating resolution and pattern fidelity limitations. The FESEM micrographs in Figure 1(a–c) illustrate the lithographic

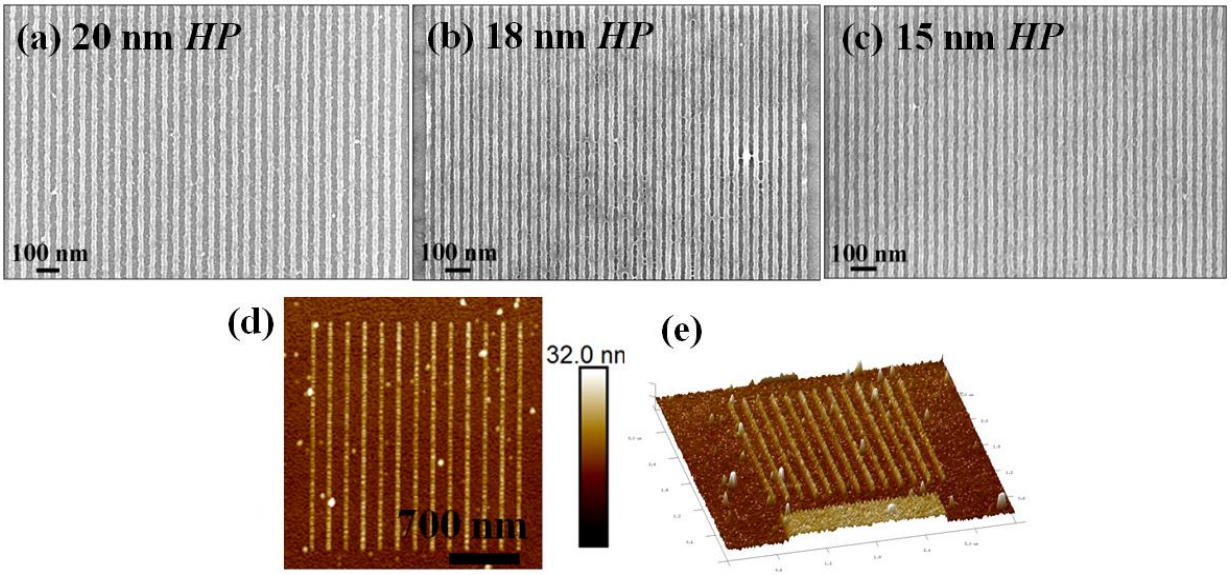

Figure 1. FESEM micrographs of R1 resist patterns generated using EBL, showing (a) 20 nm half-pitch (HP), (b) 18 nm HP, and (c) 15 nm HP line patterns. AFM micrographs of 15 nm HP line patterns of R1 resist: (d) planar view and (e) 3D topographical representation, illustrating surface morphology and pattern fidelity.

performance of the R1 resist, showing 20 nm, 18 nm and 15 nm HP line-patterns exhibited significant bridging and resist residue between features, suggesting challenges in achieving high-resolution pattern definition using R1 resist formulations. The resist residue after pattern development can also be observed in the AFM micrographs captured for 15 nm isolated line patterns [Figure 1(d-e)]. The developed patterns exhibited visibly pronounced pattern roughness, which could impact critical dimension (CD) control and overall lithographic performance. These lithography performance of R1 resist (pristine In-mTA) formulation confirms the requirement for improvement in the resist sensitivity and pattern development.

3.1.2 Enhanced Performance with 2-Iodopropane incorporations in resist formulations (R2 and R3 Resists)

The incorporation of 2-iodopropane into the resist formulation R2 and R3, serving as an iodine source, enhanced lithographic performance by increasing the resist's sensitivity to electron beam exposure. Additionally, the presence of iodine facilitated improved pattern development by promoting the dissolution of unexposed resist in the developer solution. This enhancement in solubility contributed to more efficient resist clearing, leading to improved contrast and development fidelity in the final patterned structures.

The R2 resist, incorporating 2 v/v% 2-iodopropane into the In-mTA resist formulation, exhibited well-resolved 18 nm and 15 nm half-pitch (HP) line patterns when patterned using EBL at an exposure dose of approximately 870 μC/cm^2, as shown in Figure 2(a) and (b). However, R2 was unable to achieve high-resolution patterning for dense 13 nm HP line structures [Figure 2(c)], suggesting limitations in resolution and pattern fidelity at ultra-fine dimensions in the case of R2 resists. As depicted in Figure 2(d–e), the AFM analysis corroborates the enhancement in resist pattern development attributed to the incorporation of 2 v/v% 2-iodopropane. This improvement is likely due to increased resist sensitivity and more efficient dissolution kinetics of the unexposed regions, leading to better LER measures as ~ 5.32 nm for the 15 nm HP line patterns and reduced residual defects, as observed in high-resolution lithography studies.

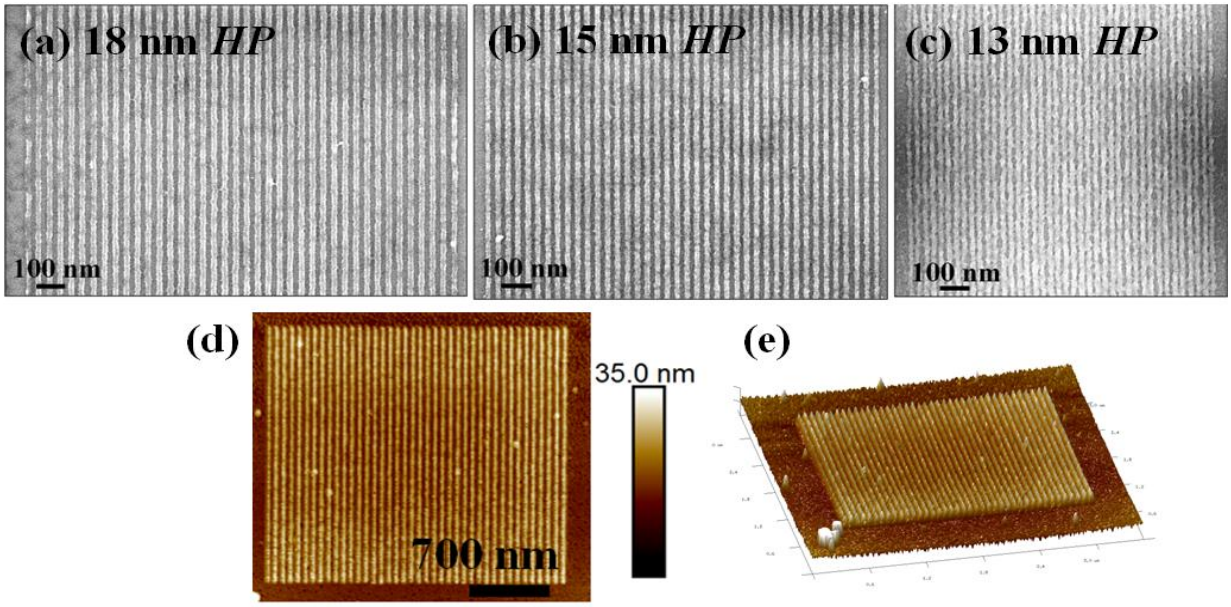

Figure 2. FESEM micrographs of R2 resist patterns generated using EBL, depicting (a) 18 nm half-pitch (HP), (b) 15 nm HP, and (c) 13 nm dense line patterns. AFM micrographs of 15 nm HP line patterns of R2 resist: (d) planar view, and (e) 3D topographical micrograph, illustrating surface morphology and pattern fidelity.

When the R3 resist, incorporating 4 v/v% 2-iodopropane in the In-mTA resist formulation, was exposed to an electron beam, it successfully generated sub-20 nm line patterns at an exposure dose of 852 μC/cm^2. Figure 3(a–c) shows that the resist demonstrated well-resolved 18 nm, 15 nm, and 13 nm half-pitch (HP) line patterns. The measured line-edge roughness (LER) for the 15 nm HP and 13 nm HP line patterns was 4.33 nm and 4.72 nm, respectively. The Lithographic performance analysis of the R3 resist under EBL indicates that incorporating 2-iodopropane significantly enhances resist sensitivity due to the presence of iodine, which facilitates electron beam interaction and energy absorption. Additionally, the iodine-functionalized resist formulation improves pattern development by increasing the solubility of the unexposed

resist in the developer solution. This enhancement leads to better pattern fidelity and reduced LER compared to the R2 resist, further demonstrating the beneficial role of iodine-containing additives in improving resolution and pattern quality in high-resolution lithography.

The lithographic performance analysis clearly demonstrates that the R3 resist outperforms its counterparts, R1 and R2. R3 exhibits higher sensitivity to electron beam exposure, requiring approximately 1.187 times lower EBL exposure dose than R1 and 1.021 times lower dose than R2, indicating enhanced energy absorption and improved patterning efficiency.

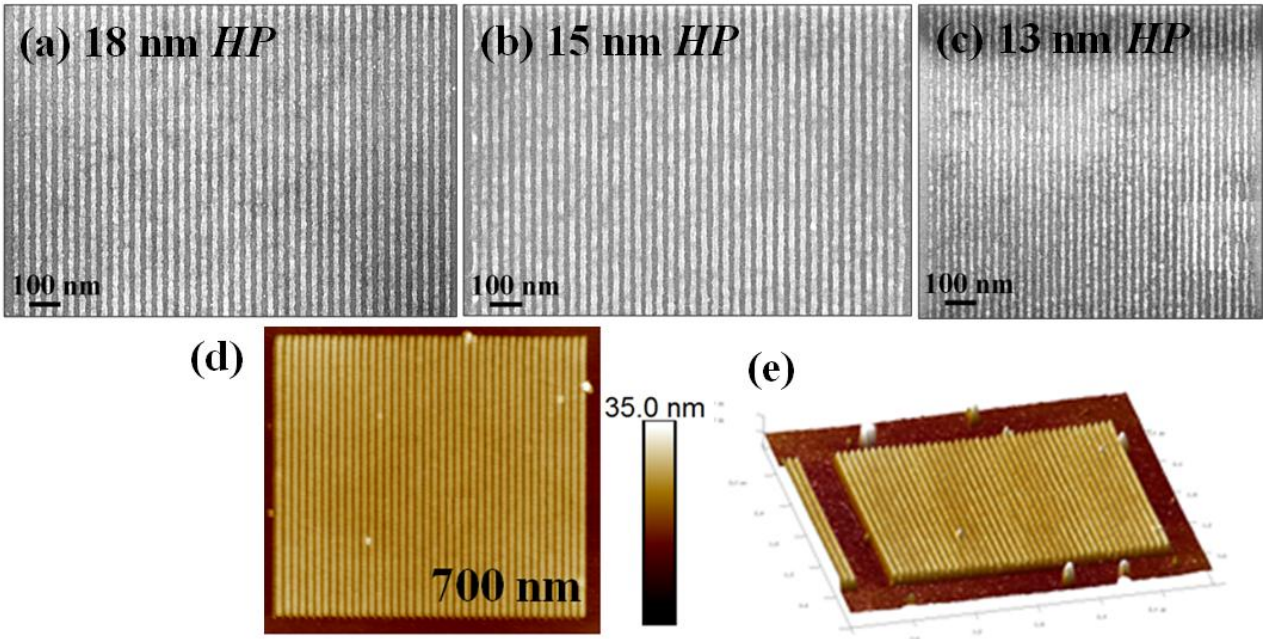

Figure 3. FESEM micrographs of R3 resist patterns fabricated using EBL, depicting (a) 18 nm half-pitch (HP), (b) 15 nm HP, and (c) 13 nm dense line patterns. AFM micrographs of 15 nm HP line patterns of R3 resist: (d) planar view, and (e) 3D topographical micrograph, illustrating surface morphology and pattern fidelity.

Furthermore, the measured LER for R3 at 15 nm and 13 nm HP line patterns falls within an acceptable range, suggesting better pattern fidelity and reduced roughness compared to R1 and R2. To further evaluate its capability in achieving sub-13 nm HP line patterns, R3-coated samples were subjected to HIBL. The resulting helium ion beam-induced line patterns of 15 nm HP, 13 nm HP and 10 nm HP are presented in Figure 4(a-c), demonstrating the potential of R3 for next-generation high-resolution sub-10 nm lithographic applications. The measured LER for 15 nm, 13 nm, and 10 nm HP line patterns generated using HIBL are 3.85 nm. 3.79 nm, and 4.01 nm, respectively.

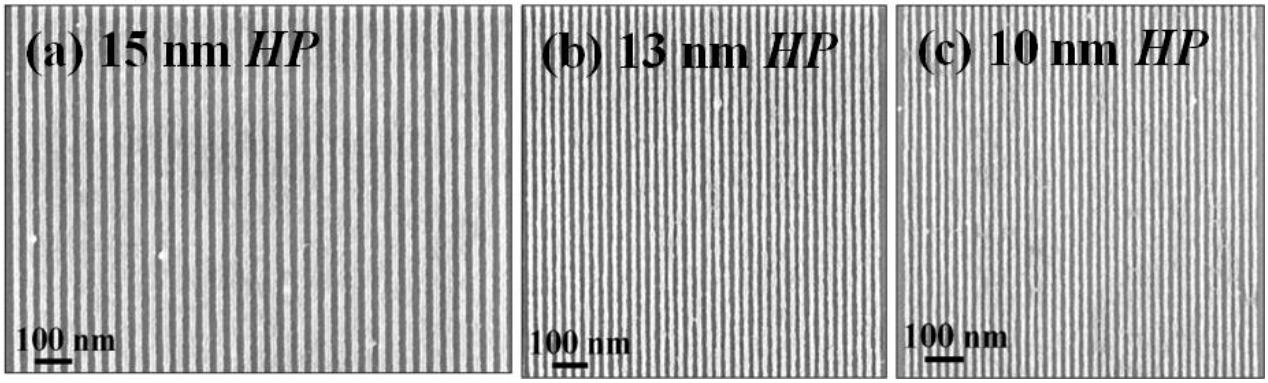

Figure 4. FESEM micrographs of R3 resist patterns fabricated using HIBL, showing (a) 15 nm half-pitch (HP), (b) 13 nm HP, and (c) 10 nm HP line patterns, demonstrating high-resolutionSub-10 nm patterning capabilities.

Contrast curve analysis is also one of the crucial parameters in evaluating resist performance, as it provides insights into resolution, edge sharpness, and pattern development. A higher contrast value ($\gamma > 2$) is generally desirable for high-resolution nanolithography, as it ensures steeper dissolution profiles, better line-edge definition, and lower LER[8]. The contrast curve analysis of In-mTA MOC resist formulations—R1, R2, and R3—was conducted by exposing 500 nm^2 area blocks under an 18 keV electron beam across the 100 to 1000 $\mu C/cm^2$ dose range. For e-beam exposure, the calculated contrast (γ) values were 1.021 for R1, 1.08 for R2, and 1.27 for R3. As shown in Figure 5(a), which presents the contrast curves for these resists, R3 exhibits the highest contrast, indicating superior pattern development compared to R1 and R2. Furthermore, the influence of e-beam and He^+ beam exposure on the contrast of R3 resist was investigated by irradiating 500 nm^2 area blocks under a 30 keV He^+ beam with doses ranging from 2 to 100 $\mu C/cm^2$. The corresponding contrast curves are depicted in Figure 5(b). Under both EBL and HIBL, the R3 resist formulation exhibited contrast values greater than 1, specifically γ_HIBL = 1.54 and γ_EBL = 1.27. This suggests improved contrast in HIBL compared to EBL, likely due to the higher energy deposition and localized interaction of helium ions with the resist, leading to a more distinct solubility gradient between exposed and unexposed regions[9]. While γ_EBL = 1.27 is moderate, it may still require further process optimization (such as post-exposure baking or developer tuning) to enhance contrast and achieve sub-10 nm patterning capabilities.

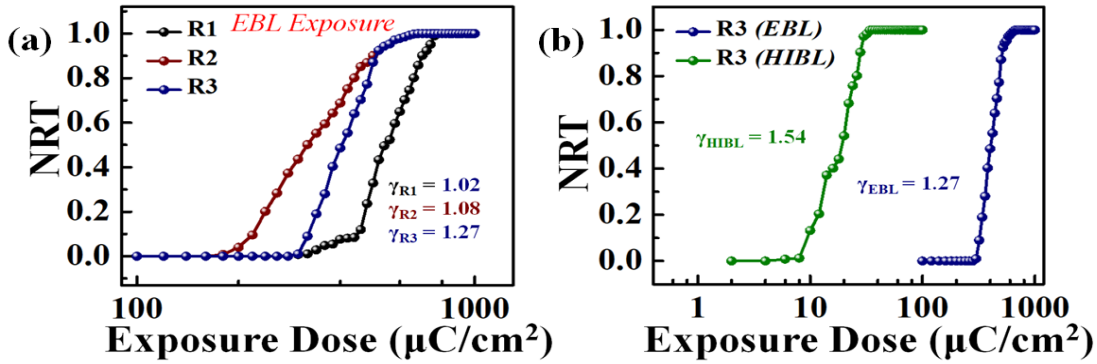

Figure 5. Normalized Remaining Thickness (NRT) vs. exposure dose for contrast measurement: (a) Comparison of R1, R2, and R3 resists exposed under EBL, and (b) Contrast analysis of R3 resist exposed under both EBL and HIBL, illustrating differences in resist response to varying exposure conditions.

3.2 FTIR of In-mTA MOC resist formulations

The FTIR absorption spectrum of In-MTA as a thin film exhibits characteristic vibrational bands. The peak at 546 cm-1 was attributed to the In-O linkage in the metal-organic complex (MOC)[10]. The broad spectral region between 1500-1300 cm^{-1} was associated with various chelating and bridging carboxylate stretching modes and asymmetric and symmetric CH_x deformation modes[11]. The peak observed at 1568 cm-1 indicated the presence of bonded carbonyl, attributed to the asymmetric stretching of the carboxylate (COO) in a bidentate coordination mode.

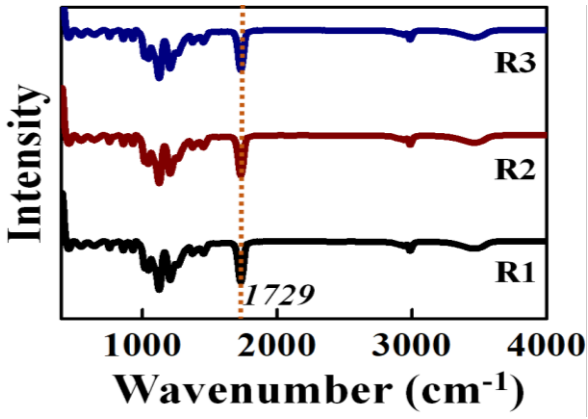

Figure 6. FTIR spectra of the formulated In-mTA resists, comparing pristine In-mTA MOC resist (R1), 2 v/v% 2-iodopropane incorporated resist (R2), and 4 v/v% 2-iodopropane incorporated resist (R3), highlighting characteristic functional group vibrations

The FTIR spectrum of the In-MOC resist exhibits a characteristic absorption band at 1729 cm^{-1}, corresponding to the stretching vibrations of the carbonyl (C=O) group in the ester linkage of the ligand coordinated with indium metal. Upon doping with iodopropane in the resist solution (R1), this band undergoes a slight shift toward a higher wavenumber at 1730 cm-1. This shift indicates an interaction between iodine and the carbonyl functional group, likely altering the electron density around the C=O bond and affecting the chemical environment of the resist, potentially enhancing its structural stability and sensitivity. Additionally, the bending vibration of C=C bonds of aromatic alkenes was observed at 1452 cm^{-1}, while the peak at 2985 cm^{-1} corresponds to the stretching of aromatic alkene (═C-H) groups. The broader peak in the region of vibration stretching at 3466 cm-1 was attributed to the -OH group present in the solvent ethyl lactate.

4. CONCLUSIONS

In summary, the incorporation of 2-iodopropane into In-mTA metal-organic cluster (MOC) resist formulations has remarkably elevated their lithographic performance, unlocking unparalleled levels of sensitivity, contrast, and pattern fidelity. Among the various formulations evaluated, R3 stands out with excellent results, achieving sub-15 nm half-pitch line patterns through EBL and down to 10 nm line patterns via HIBL. Not only does R3 excel with a lower line edge roughness (LER), but it also requires less exposure dose while delivering higher contrast. Further analysis of the contrast curves underscores R3's superior resolution, particularly under HIBL, showcasing a significant advantage in contrast and sensitivity over EBL. These compelling results underscore the transformative potential of MOC-based resists in the realm of next-generation nanolithography, particularly for achieving sub-10 nm patterning in extreme ultraviolet (EUV) lithography and beyond. The future of advanced lithography is bright, with MOC technology at the forefront.

ACKNOWLEDGMENT

The authors express their gratitude to Merck: EMD Electronics & EMD Performance Materials Corp., 70 Meister Ave, Somerville, NJ 08876, Intreid Avenue, Suite 300, Philadelphia, PA 19112, USA, for funding and the Centre for Design and Fabrication of Electronic Devices (C4DFED) at the Indian Institute of Technology (IIT) Mandi, India, for providing access to the Class 100 cleanroom facility and various advanced instruments used in this study. They acknowledge the use of Zeiss Orion NanoFab (HIBL) and Raith e-Line PLUS (EBL) patterning systems for lithography, as well as the Zeiss Gemini SEM 500 (FESEM) for imaging, all available at the C4DFED facility at IIT Mandi.

REFERENCES

[1] Xu, H., Kosma, V., Giannelis, E., Ober, C. K. and Sakai, K., "EUV photolithography: resist progress and challenges," SPIE **1058306**(March 2018), 2 (2018).

[2] De Simone, D., Vanelderen, P. and Vandenberghe, G., "Photo material readiness at the eve of EUVL HVM," J. Photopolym. Sci. Technol. **30**(5), 613–617 (2017).

[3] Sharma, S., Kumar, R., Chauhan, M., Moinuddin, M. G., Peter, J., Ghosh, S., Pradeep, C. P. and Gonsalves, K. E., "All new nickel based Metal Core Organic Cluster (MCOC) resist for N7+ node patterning," SPIE **1132604**(March), 3 (2020).

[4] Sharma, S. K., Chauhan, M., Kumar, R., Palit, K., Choudhary, S. and Gonsalves, K. E., "Development of metal-organic cluster based negative tone resist: pre-screened through the helium-ion beam prelude to extreme ultraviolet lithography (EUVL) applications," SPIE **1161208**(February), 7 (2021).

[5] Xu, H., Sakai, K., Kasahara, K., Kosma, V., Yang, K., Herbol, H. C., Odent, J., Clancy, P., Giannelis, E. P. and Ober, C. K., "Metal-organic framework-inspired metal-containing clusters for high-resolution patterning," Chem. Mater. **30**(12), 4124–4133 (2018).

[6] Chauhan, M., Palit, K. and Choudhary, S., "Ultrasensitive metal-organic cluster resist for patterning of single exposure high numerical aperture extreme ultraviolet lithography applications," J. Micro/Nanopatterning, Mater. Metrol. **21**(4), 1–17 (2022).

[7] Fallica, R., Haitjema, J., Wu, L., Castellanos, S., Brouwer, F. and Ekinci, Y., "Absorption coefficient and exposure kinetics of photoresists at EUV," SPIE **10143**(March 2017), 101430A (2017).

[8] Kozawa, T., Tagawa, S., Santillan, J. J., Toriumi, M. and Itani, T., "Image contrast slope and line edge roughness of chemically amplified resists for postoptical lithography," J. Vac. Sci. Technol. B Microelectron. Nanom. Struct. Process. Meas. Phenom. **25**(6), 2295–2300 (2007).

[9] Ruchhoeft, P. and Wolfe, J. C., "Determination of resist exposure parameters in helium ion beam lithography:

Absorbed energy gradient, contrast, and critical dose," J. Vac. Sci. Technol. B Microelectron. Nanom. Struct. Process. Meas. Phenom. **18**(6), 3177–3180 (2000).
[10] Jothibas, M., Manoharan, C., Johnson Jeyakumar, S. and Praveen, P., "Study on structural and optical behaviors of In2O3 nanocrystals as potential candidate for optoelectronic devices," J. Mater. Sci. Mater. Electron. **26**(12), 9600–9606 (2015).
[11] Mattson, E. C., Cabrera, Y., Rupich, S. M., Wang, Y., Oyekan, K. A., Mustard, T. J., Halls, M. D., Bechtel, H. A., Martin, M. C. and Chabal, Y. J., "Chemical Modification Mechanisms in Hybrid Hafnium Oxo-methacrylate Nanocluster Photoresists for Extreme Ultraviolet Patterning," Chem. Mater. **30**(17), 6192–6206 (2018).